The Impact of Enzymatic Degradation on the Uptake of Differently Sized Therapeutic Molecules

ARNE ERIKSON[1], INGUNN TUFTO[1], ANNE BERIT BJØNNUM[1],
ØYVIND S. BRULAND[2] and CATHARINA DE LANGE DAVIES[1]

[1]*Department of Physics, Norwegian University of Science and Technology, Høgskoleringen 5, 7491 Trondheim;*
[2]*University of Oslo, Department of Oncology, The Norwegian Radium Hospital, N-0310 Oslo, Norway*

Abstract. *Background: The extracellular matrix represents a major barrier for drug delivery. This work compares the effects of collagenase and hyaluronidase on tumour uptake and distribution of two differently sized therapeutic molecules, IgG and liposomal doxorubicin. Materials and Methods: The enzymes were injected i.v. prior to the therapeutic molecules, and uptake and distribution were studied by confocal laser scanning microscopy. The therapeutic molecules were colocalized with the vasculature and collagen network visualized by the second harmonic signal. Results: Hyaluronidase increased the uptake of liposomal doxorubicin to a small extent, whereas collagenase had no effect. Collagenase increased, but hyaluronidase reduced the uptake of IgG. Neither of the enzymes induced changes in the collagen network measured by the second harmonic signal. Conclusion: Degradation of the collagen network improves delivery of molecules with the size of IgG, whereas degradation of the gel of glycosaminoglycans has a higher impact on the distribution of small drugs such as doxorubicin.*

Advances in nanomedicine have led to the design of an increasing number of therapeutic anticancer agents such as monoclonal antibodies, liposomes and nanotechnology-based delivery systems that offer unique opportunities compared with traditional chemotherapeutic agents. One major advantage is cancer cell specificity, resulting in significantly less harm to normal cells. However, a systemically administered nanomedicine may not reach its target due to barriers en-route, mainly because of the relatively large size of such agents. The transport of therapeutic molecules in tumour tissue is governed by convection and diffusion (1). Due to the high interstitial fluid pressure (IFP) in tumours (2-4), diffusion may be the major transport mechanism. However, diffusion is a very slow process for larger molecules that have to penetrate the extracellular matrix (ECM), which consists of a structural collagen network embedded in a gel of glycosaminoglycans. Recent studies have investigated the relative roles played by key ECM molecules in transport hindrance (5-9). The results point to collagen as a major determinant of resistance to drug transport in solid tumours, but glycosaminoglycans and proteoglycans may also be of importance. Hence the interactions between collagen and proteoglycans give rise to significant interstitial transport resistance (5, 10).

One strategy for enhancing transport properties through the ECM is the use of enzymes to degrade the hindering molecules. Studies have shown that significant transport improvements could be achieved after pretreatment with matrix metalloproteinases (MMPs) such as collagenase or with hyaluronidase (4, 9, 11-13). However, a direct comparison between the effects of collagenase and hyaluronidase on the uptake and distribution of differently sized therapeutic molecules is lacking. The purpose of the present work was therefore to address these shortcomings by comparing the effects of collagenase and hyaluronidase on tumour uptake and distribution of immunoglobulins (IgG) and liposomal doxorubicin. This was achieved by intravenous (*i.v.*) injection of the enzymes prior to the therapeutic molecules, and the uptake and distribution was studied by confocal laser scanning microscopy. The distribution of the therapeutic molecules was colocalized with the vasculature and the collagen network was visualized by the second harmonic signal (SHG).

Materials and Methods

Tumour models. The human osteosarcoma cell line OHS (14) was grown as xenografts in female athymic BALB/c nu/nu mice, (Taconic M&M, Ry, Denmark) orthotopically or in dorsal skinfold window chambers. Orthotopic tumours were established by injecting 30 μl/2$\times10^6$ cells adjacent to the periosteum of the femurs in 7- to

Correspondence to: C. de L. Davies, Department of Physics, The Norwegian University of Science and Technology, Høgskoleringen 5, 7491, Trondheim, Norway. Tel: +47 73593688, email: catharina.davies@ntnu.no

9-week-old mice (15). The xenografts were grown for 3-6 weeks and the tumour sizes ranged from 500 to 1,500 mm^3.

Dorsal skinfold window chambers were implanted on the back of 10- to 16- week-old mice as described by Endrich *et al.* (16). Briefly, an extended double layer of skin was sandwiched between two symmetrical titanium frames (Institute for Surgical Research, Ludwig Maximillans University, Munich, Germany) and a circular area of 15 mm in diameter from one layer of skin was completely removed. The remaining layers of the other skinfold (thin striated skin muscle, subcutaneous tissue, dermis and epidermis) were covered with a glass coverslip incorporated into one of the titanium frames. Twenty-four hours after the implantation of the chamber, the coverslip was removed and 1.5×10^6 OHS cells were injected into the centre of the chamber. A new coverslip was placed above and the chamber closed. The tumours were grown for 19-24 days; the animals tolerated the chamber well and they showed no signs of discomfort.

The mice were anaesthetized by a subcutaneous (*s.c.*) injection of Fentanyl/Midazolam/Haldol/sterile water (3:3:2:4) 10 ml/kg body weight (Hameln Pharmaceuticals, Germany; Alpharma AS, Norway; and Janssen-Cilag AS, Norway, respectively). All surgical procedures were performed under sterile conditions. The animals were kept under pathogen-free conditions at a constant temperature (24-26˚C) and humidity (30-50%) and were allowed food and water *ad libitum*. All animal experiments were carried out with Ethical Committee approval. The ethical guidelines that were followed meet the standard required by the UKCCCR guidelines.

Therapeutic molecules. Liposomal doxorubicin (Caelyx™; Schering Plough, Norway) with a diameter of approximately 96 nm was injected into the tail vein in mice bearing orthotopic tumours. A volume of 200 μl of 16 mg/kg was injected. The osteosarcoma-associated monoclonal antibody TP-3 (IgG 2b) (17) was injected *i.v.* in mice bearing either orthotopic tumours or tumours in dorsal chambers. TP-3 was developed in response to immunization of mice with osteosarcoma cells and binds to a specific epitope on a M_w 80,000 monomeric polypeptide cell-surface membrane antigen. TP-3 was conjugated to Alexa Fluor 488 using the Alexa Fluor 488 Protein Labeling Kit (Molecular Probes, Eugene, Oregon, USA).

Treatments of tumours. The ECM-degrading enzymes collagenase and hyaluronidase were used to modulate the collagen and hyaluronan content and structure of the tumour tissue. Collagenase (0.1% w/v 100 μl; 233 units/mg, Clostridiopeptidase A; Sigma, St. Louis, MO, USA), hyaluronidase (1500 U 100 μl, Hylase Dessau; Riemser Arzneimittel AG, Greifswald-Insel Riems, Germany) or phosphate-buffered saline (PBS) (100 μl) was injected *i.v.* into the tail vein. The doses were chosen based on previous work demonstrating that these doses induced maximum reduction in IFP (4, 12).

At 100 minutes after enzyme administration, either liposomal doxorubicin or the TP-3 antibody was injected. This time point was based on previous results demonstrating that enzymatic treatment induced a transcapillary pressure gradient at this time point (4, 12).

In orthotopically growing tumours, the blood vessels were visualized by injecting Hoechst 33342 (14 mg/kg bodyweight 100 μl; Molecular Probes) 5 min before sacrificing the mice by cervical dislocation. The mice were sacrificed 1 or 24 h after the enzymatic treatment. The tumours were excised, embedded in Tissue Tec (O.C.T., Histolab Products, Göteborg, Sweden), frozen in liquid nitrogen and stored at –80˚C. Frozen sections, 5 μm-thick, were cut evenly separated through each tumour and mounted on glass slides.

In tumours growing in dorsal skinfold window chambers, the blood vessels were visualized by *i.v.* injection of 2 MDa tetramethyl rhodamine dextran (TMR-dextran, 15 mg/ml, 100-150 μl; Molecular Probes). In addition to the enzymatic treatment described above, a higher concentration of collagenase (0.3%, 100 μl) was injected *i.v.* Removal of the dorsal skinfold window chamber coverslip and adding 50 μl collagenase (1%, 2% and 5%) was also performed to study enzymatic effects on the collagen network.

Confocal laser scanning microscopy. The uptake and distribution of therapeutic molecules, the localization of tumour vessels and interstitial collagen were studied using confocal laser scanning microscopy (CLSM) (LSM Meta 510; Zeiss, Jena, Germany) with a Plan-Neofluar 20x/0.5 (sections of orthotopic tumours) or a C-Achroplan 40x/0.8W Corr objective (dorsal skinfold window chamber tumours). A 488 nm laser line was used to excite doxorubicin and TP-3-Alexa Fluor 488, a 543 HeNe laser was used to excite the TMR-dextran, a mode-locked Ti:Sapphire laser (Mira Model 900-F; Coherent, Inc., Laser Group, Santa Clara, Ca, USA) was used at λ=780 nm to excite Hoechst 33342, and at λ=810 nm to generate SHG signal from collagen. For tumour tissue, the optimal excitation wavelength to generate SHG signal from collagen has previously been found in the range 800-810 nm (18). SHG signals were detected in the transmitted light direction (sections of orthotopic tumours) and in the backscattered direction (dorsal skinfold window chamber tumours). A bandpass filter (385-425 nm) was placed in front of the SHG detector to exclude light from the incoming laser.

In vivo studies of dorsal skinfold window chamber tumours were performed by placing the anaesthetized mice on a heating pad at 37˚C which was fixed to the microscope table in a specially built mouse holder. Several positions in the tumour were located prior to any enzymatic treatment, where the criterion for position selection was identification of chaotic blood vessels and a well-defined SHG signal. These positions were relocated when monitoring effects 100 min and 24 h following the enzymatic treatment.

Image analysis. The uptake of liposomal doxorobicin and TP-3 was quantified by calculating the % area of fluorescence in images of tissue sections (*i.e.* the number of pixels in an image with fluorescence divided by the total pixel number in that image ×100). Images were thresholded identically within the same treatment groups, using built-in software (LSM Meta 510; Zeiss). Free doxorubicin released from the liposomes, and Alexa Fluor 488 were the fluorophores detected. Intact liposomes were not imaged. Frozen sections were imaged along a radial track from the periphery through the centre and to the periphery on the other side of each tumour section. In all, 10 to 24 images were recorded per section, depending on the position within the tumour and the size of the tumour. This was performed for 4 to 5 sections per tumour and 4 to 6 tumours per treatment group. The sections were 400 μm apart, with the first section being approximately 250 μm from the tumour periphery. Autofluorescence from unstained sections was not detectable with the instrument settings used.

TP-3 uptake in tumours growing in dorsal skinfold window chambers was quantified by measuring % area of fluorescence in identically thresholded images 15-30 min after TP3 administration (ImageJ, U.S. NIH, Bethesda, MD, USA). A total of 3 to 12 images was analysed in the different groups.

SHG signals from collagen fibres were collected from peripheral, semi-peripheral and central positions of frozen tumour sections 1 and 24 h after enzymatic treatment. Ten to twenty images were

recorded from 5 sections per tumour and 3-4 tumours per treatment group. SHG signals from collagen fibres in tumours in dorsal skinfold window chambers were studied 0 h, 100 min and 24 h after treatment. *z*-Stacks consisting of 3-8 images spaced 3 μm apart were generated in 2 to 3 mice from each treatment group, using 1 to 4 positions in each mouse. Maximum intensity projections were generated from the *z*-stacks and were the basis for quantifying the parameters named below.

The collagen fibres were described by three parameters: (i) % area of collagen, (ii) entropy and (iii) skewness. Collagen content in the images (% area) was quantified estimating the area with SHG signal in thresholded images using automated software algorithms (ImageJ; U.S. NIH, Bethesda, MD, USA). Collagen structure was quantified measuring the image texture descriptor entropy defined as

$$E = - \sum_{i=0}^{L-1} p(z_i) \log_2 p(z_i)$$

(19). This is a measure of randomness indicating whether the collagen is more or less ordered in a chosen region of interest (ROI), where randomness and order are reflected by high and low entropy, respectively. Typical values of high and low entropy are 7.8 and 6.5 (19). z_i Is a random variable indicating intensity, *p(z)* is the histogram of the intensity levels in the ROI, and *L* is the number of intensity levels in the ROI. In the analysis of tumour collagen structure, each image was subdivided into 256 ROIs of size 32×32 pixels giving 256 entropy values per image. The maximum of these values was used for further analysis, as the mean was approximately the same in all images and the minimum was the entropy of subimages with black pixels only.

Skewness and entropy were measured in nonthresholded images. Skewness is a measure of the asymmetry of the data around the sample mean. The skewness of a normal distribution is 0. Positive or negative skewness values represent data spread out more to the right or to the left, respectively.

Statistics. Statistical comparison of data (Minitab, Minitab Inc., State College, PA, USA) of the uptake of TP-3 or liposomal doxorubicin in orthotopic tumours was performed by nonparametric analysis using the Mann-Whitney test. Statistical analysis of the Gaussian uptake data of TP-3 in tumours in dorsal skinfold window chambers was performed using a two-sample *t*-test.

To determine the degree of hindrance the collagen network represents, a Chi-square analysis and Fisher's exact test of contingency tables were performed. The variables in the test were: i) collagen network (loose or well-defined), ii) tumour treatment (collagenase, hyaluronidase, or none) and iii) penetration of therapeutic macromolecule (yes or no). Values in the text are stated as mean ± standard error. All the statistical analyses were performed using the significance criterion of $p \leq 0.05$.

Results

Effects of hyaluronidase and collagenase on uptake and distribution of liposomal doxorubicin and TP-3 in orthotopic tumours. Hyaluronidase increased the uptake of liposomal doxorubicin in orthotopic tumours to a small extent, whereas collagenase had no effect. The median value for the % area of doxorubicin fluorescence released from liposomes was significantly higher (~4%) for hyaluronidase- compared

with collagenase- and untreated tumours (Figure 1, upper row). Collagenase increased (~10%) but hyaluronidase reduced (~10%) the uptake of the monoclonal antibody TP-3 as compared with the control (untreated) with significant differences between all three groups (Figure 1, lower row). The uptake of the therapeutic agents was rather low, approximately 20-25% and 40-50% of the tumour tissue showed uptake of liposomal doxorubicin and TP-3 antibody, respectively. Comparing the uptake in the periphery, semi-periphery and central part of the tumours, no significant differences were observed, and the enzymatic effect was the same in the three tumour locations. The data and images in Figure 1 are thus representative of the whole tumour.

As shown in Figure 1, the distribution of both liposomal doxorubicin and TP-3 antibody was heterogeneous both in treated and untreated tumours. The doxorubicin was generally distributed further away from the blood vessels in hyaluronidase-treated mice. Significantly improved distribution at all tumour locations was detected for the monoclonal antibody TP-3 after collagenase administration compared with hyaluronidase- and untreated tumours, and penetration further away from the blood vessels was clearly observed.

Effects of hyaluronidase and collagenase on collagen network in orthotopic tumours. The collagen fibre network was visualized by the SHG signal. The content of collagen fibres type I was determined by the % area of SHG signal in images of frozen sections of treated and untreated tumours (Figure 2, upper row). One hour after treatment, a significantly higher % area was found in the periphery (~400 μm into the tumour) of hyaluronidase-treated tumours compared with collagenase-treated tumours, whereas no differences were found between the groups at semi-peripheral or central locations. After 24 h, a significantly higher % area was found in both the periphery and the centre of collagenase-treated tumours compared with hyaluronidase- and untreated tumours. Comparing the two times, the most significant differences can be seen at the tumour periphery: An increase (~2 fold) and a decrease (~1/2) in % area were observed after 24 h in collagenase- and hyaluronidase-treated tumours, respectively, compared with areas at 1 h.

In order to quantify structural changes in fibrillar collagen, the image texture descriptor entropy was used (Figure 2, middle row). Entropy reflects a random distribution of pixel values, with higher values reflecting a more disordered collagen structure. A clear tendency towards lower entropy values (25% reduction) was found when proceeding through the tumours from the periphery to the centre. This finding applied to all groups (treated and untreated) and times (1 and 24 h after enzymatic treatment). No significant differences were found between the groups or the times.

The statistical parameter skewness was measured showing significant differences comparing collagenase- and hyaluronidase-treated tumours at all locations and times with
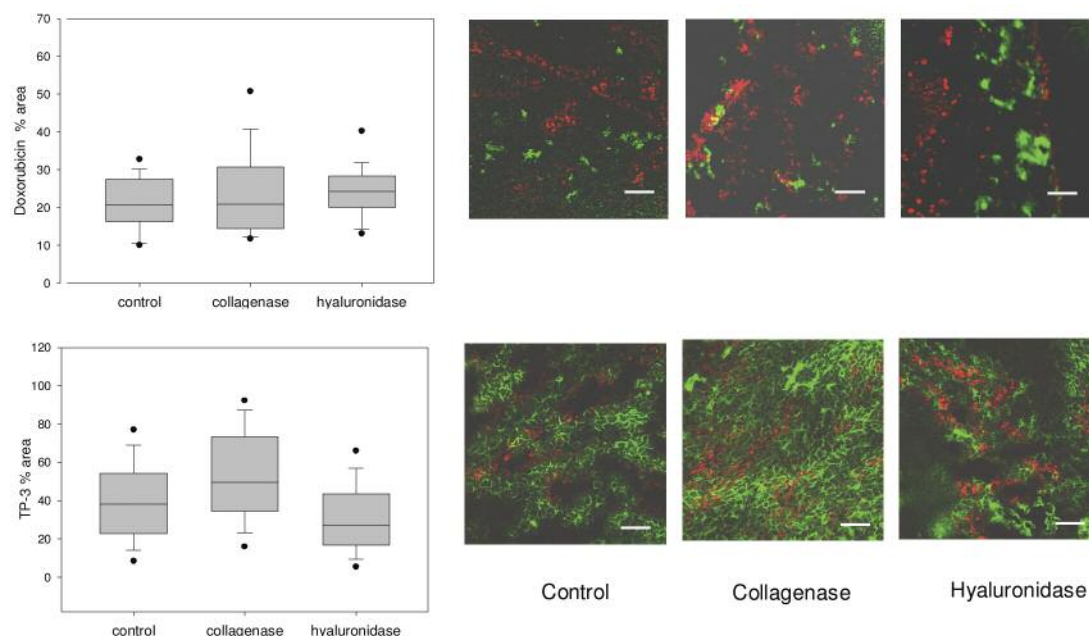
Figure 1. *Boxplots: % Area of liposomal doxorubicin (top) and TP-3 IgG (bottom) fluorescence in untreated (control), collagenase-, or hyaluronidase-treated orthotopic tumours. Mid-horizontal lines in boxes represent median values. The other markings from bottom up represent: 5th (point), 10th (whisker), 90th (whisker) and 95th (point) percentiles. n=5-6 (doxorubicin), n=4 (TP-3) tumours in each group and 5 sections were analysed for each tumour. The uptake was recorded 24 h after treatment. Images: Distribution of liposomal doxorubicin (green) and TP-3 (green) after no (control), collagenase, or hyaluronidase treatment in the central part of tumours. Red represents staining of blood vessels. Scale bar=50 μm.*

one exception (semi-periphery, 1 h) (Figure 2, lower row). No differences were found between hyaluronidase- and untreated tumours. Comparing collagenase- and untreated tumours, a significant reduction in the skewness parameter was found only in the central and semi peripheral locations 24 h after treatment. Comparing the two time points, significant differences were also observed at all tumour locations with one exception (hyaluronidase, central). Collagenase- and hyaluronidase-treated tumours decreased (by ~2/3) and increased (~1.3 fold), respectively, comparing skewness values at 1 and 24 h.

Influence of collagen structure on drug penetration. Two categories of collagen fibres, loose and well-defined collagen network, were identified in untreated and treated tumours. The various treatments did not induce significant differences in the occurrence of the two categories. Representative images are shown in Figure 3 A and B for well-defined and loose collagen network, respectively. 2×2 Contingency tables were generated for testing the effect of treatment upon liposomal doxorubicin (n=188 images) and TP-3 (n=47 images) penetration into the collagen network categories. Analyzing the contingency tables, data showed no significant differences in penetration. Interpreting penetration was achieved by visual inspection of the images where

penetration was defined as drugs lying well embedded in the collagen network. However, drugs that had penetrated through the network would not be observed in this analysis. Figure 3 C and D show images of monoclonal antibody TP-3 and liposomal doxorubicin (blue) distribution in semi-peripheral tumour location 24 h after collagenase and hydaluronidase treatment, respectively.

Effect of hyaluronidase and collagenase on distribution and uptake of TP-3 in dorsal skinfold window chambers. In order to study the uptake of therapeutic macromolecules noninvasively, the uptake of TP-3 antibody in tumour growing in dorsal skinfold window chambers was determined by estimating the % area of TP-3-Alexa Fluor 488 fluorescence. Only the uptake in the interstitium was included, and the % area was measured on identically thresholded images 15-30 min after TP-3 injection, which was given 100 min after enzyme administration. Representative images are shown in Figure 4. A significantly higher % area was found for the collagenase-treated tumours (3.8±0.7) compared with hyaluronidase-treated (0.4±0.1) and untreated tumours (0.2±0.1). No differences were found between untreated and hyaluronidase-treated tumours. Quantitative analysis of images 24 h after enzymatic treatment was inconclusive due to image noise and unidentifiable artefacts.
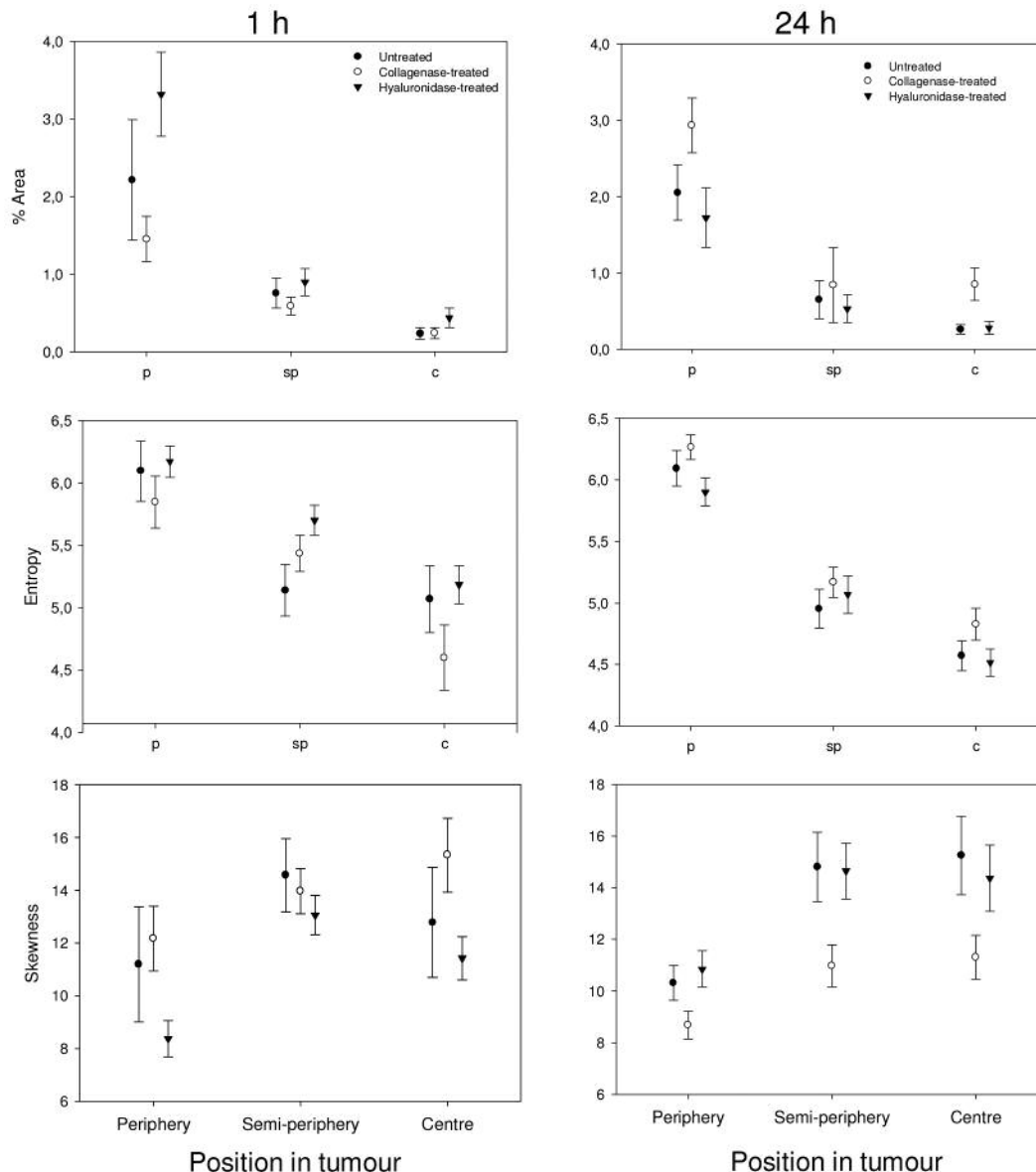
Figure 2. *Analysis of collagen network in frozen tumour sections. % Area of SHG signal, entropy and skewness values versus location in frozen sections of tumours 1 and 24 h after enzymatic treatment. N=3-4 tumours from each group; 10-20 images from different sections were recorded for each group. Bars=standard error.*

Effects of hyaluronidase and collagenase on collagen network in dorsal skinfold window chambers. The collagen structural network was studied noninvasively. This was carried out by visualisation of SHG signals from the collagen fibres in tumours growing in dorsal window chambers. In accordance with the observations on frozen sections, enzymatic degradation did not induce any visible changes (Figure 5). To further study if enzymatic treatment had induced changes in the amount of collagen fibre, or any structural changes, the images were analysed with respect to % area, entropy and skewness. Figure 6 shows these parameters *versus* imaging time after enzymatic treatment of individual mice. No significant changes were observed within experimental errors, comparing effects of enzymatic treatment at different times.

Increasing the *i.v.* collagenase concentration to 0.3% did not induce any changes in the collagen network which was monitored every hour for 3 hours (Figure 5, B). A further increase in collagenase to 0.5% was lethal (4). Removal of the glass coverslip in the dorsal window chamber and
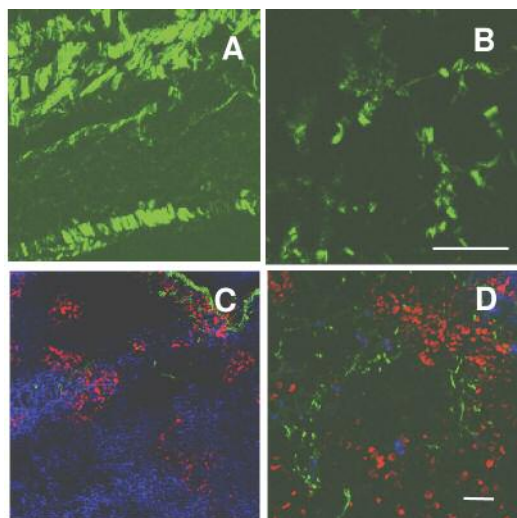
Figure 3. *Representative SHG images of well-defined (A) and loose collagen network (B). Images of monoclonal antibody TP-3 (C) and liposomal doxorubicin (blue) (D) distribution in semi-peripheral tumour location 24 h after collagenase and hydaluronidase treatment, respectively. Blood vessels (red) and collagen (green) are also shown. Scale bar=50 μm.*

applying 1% or 5% (50 μl) collagenase directly to the tumour and surrounding tissue degraded the tissue to such an extent that imaging was impossible.

Discussion

The present results may indicate that degradation of the structural collagen network is more important than degradation of the gel of glycosaminoglycans in order to improve the delivery and uptake of molecules with the size of IgG. On the other hand, degradation of the hydrophilic gel of glycosaminoglycans has a higher impact on the distribution and uptake of small drugs, such as doxorubicin released from liposomes, than does degradation of the collagen network.

The role of collagenase in transport hindrance. Collagenase had a higher impact on the delivery of the larger sized molecule IgG (TP-3) than hyaluronidase did. This was found in osteosarcoma growing both orthotopically and in dorsal window chambers.

The enhanced uptake of therapeutic molecules is due to increased diffusion (20, 21), as well as the induction of a transcapillary pressure gradient (4). Collagenase disrupts collagen at the molecular level which probably results in more available space for free movement of TP-3, whereas the collagen network does not limit the penetration of the smaller doxorubicin to the same extent and thus no effect of collagenase is apparent. Degrading the fibrillar collagen

network was previously found to improve the distribution of larger molecules compared with smaller tracers (22) and collagen content was found to correlate inversely with the diffusion coefficient of IgG (5, 8). We also found in a previous study that the fibrillar collagen content had a higher impact on enhancing diffusion than did the structure of the collagen network (23).

Although collagenase increased the penetration of IgG antibodies, the collagen network did not represent an absolute barrier. The therapeutic molecules were able to penetrate both the loose and well-defined collagen network. This is consistent with the finding that the collagen network only blocked large viral vectors and not dextran of size 2 MDa (22).

The role of hyaluronan in transport hindrance. Hyaluronidase increased the uptake and improved the distribution of liposomal doxorubicin released from liposomes. Moreover, multicellular spheroid incubation with hyaluronidase has been shown to improve the penetration of doxorubicin (24). In clinical trials, hyaluronidase was reported to improve the therapeutic outcome when given adjuvant to chemotherapy (25-27). The present work did not show any hyaluronidase-induced increase in the uptake of IgG. However, recombinant hyaluronidase has been shown to enhance the distribution of intradermally administered adenoviruses and particles with diameters less than 500 nm (28). This discrepancy may be due to differences in hyaluronidase activity and doses used.

Hyaluronidase has been reported to enhance diffusion (29), reduce interstitial fluid pressure (12) and increase the penetration through the epithelial luminal glycocalyx (30) in a nonlinear dose-dependent manner. Hyaluronidase facilitated these processes up to a certain dose, followed by a decrease, probably due to collapse of the water swelling structures of the hyaluronan. Hyaluronan interacts with the collagen network and hence collapse of the hyaluronan structures may also affect the collagen network. Although the dose of hyaluronidase used in the present study was previously reported to increase diffusion and reduce interstitial fluid pressure (12), in the present study it may have induced the above mentioned collapse, resulting in less space being available for the mobility of larger molecules.

Effect of collagenase and hyaluronidase on the collagen network. SHG imaging allowed visualization of fibrillar collagen structure both in frozen sections and *in vivo* in dorsal skinfold window chambers, and dynamic imaging was performed within a time span of 24 h. Visual and quantitative analysis of the images was unable to establish significant changes in the collagen network after collagenase and hyaluronidase treatment. Three parameters were used to quantitate the collagen network: collagen content as given by % of pixels with SHG signal; entropy, representing the degree of order of collagen fibers; and the statistical
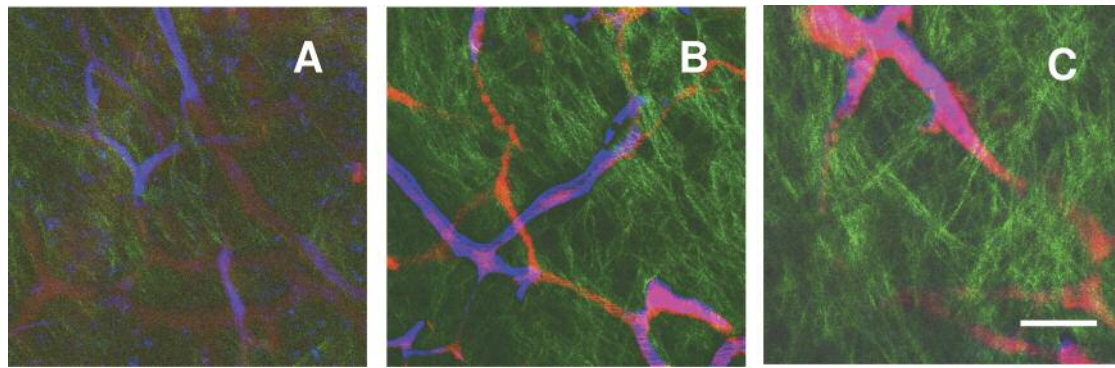
Figure 4. *Representative images of dorsal skinfold window chamber showing tumour vasculature (red, blue, pink), therapeutic macromolecule, TP-3 (blue) and collagen network (green). TP-3 was injected 100 min after enzyme administration and images recorded 15-30 min later. A, Collagenase-treated; B, hyaluronidase-treated; C, untreated. Scale bar=50 μm.*
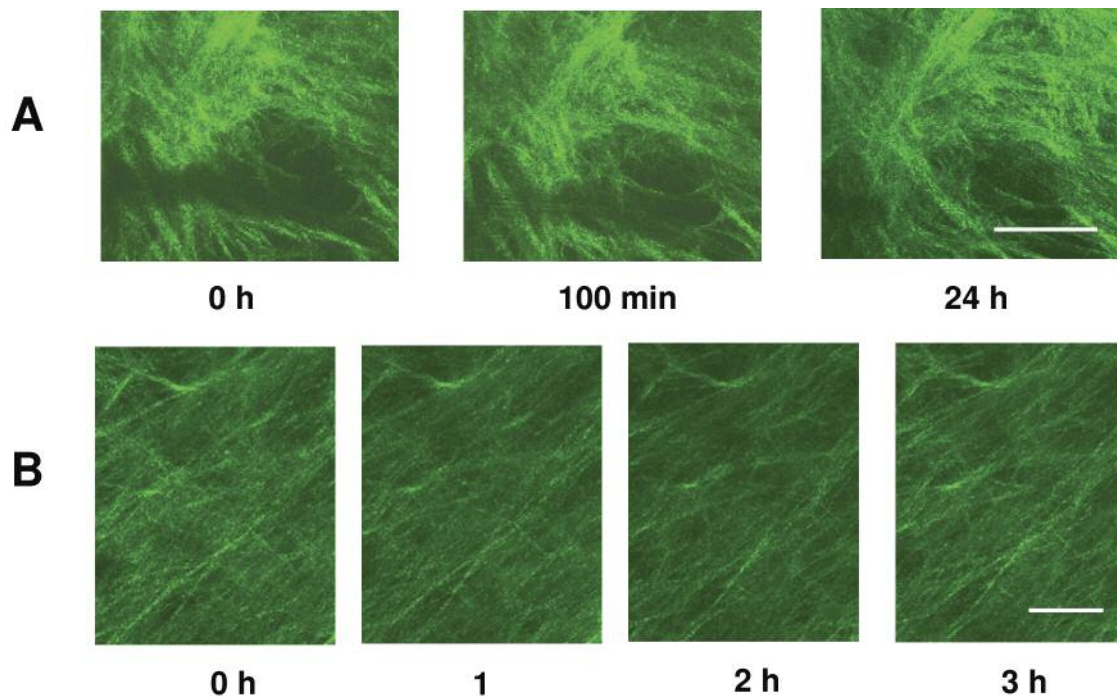

Figure 5. *Collagen network in dorsal skinfold window chambers imaged at different times after collagenase injection. A, 0.1%; B, 0.3% collagenase. Scale bar=50 μm.*

parameter skewness. Neither collagenase nor hyaluronidase induced any changes in these parameteres, except for skewness analysed on frozen sections and a small increase in collagen content 24 h after collagenase treatment. This increase probably reflects enhanced collagen resynthesis. Decreasing entropy values were found for all treatment groups when proceeding through the tumours from the periphery to the centre, reflecting a higher degree of order. This may be due to the higher occurrence of single strands of collagen fibres in the central parts compared to the denser and more connected collagen fibres detected at the periphery.

The results found in frozen tumour sections and in tumours growing in dorsal window chambers were consistent, although the tissue in dorsal window chambers had a higher collagen content. The differences in collagen content and structure between the orthotopically growing tumours and tumours in dorsal window chambers were reflected in the approximately 10-fold higher value of % area and 10-fold
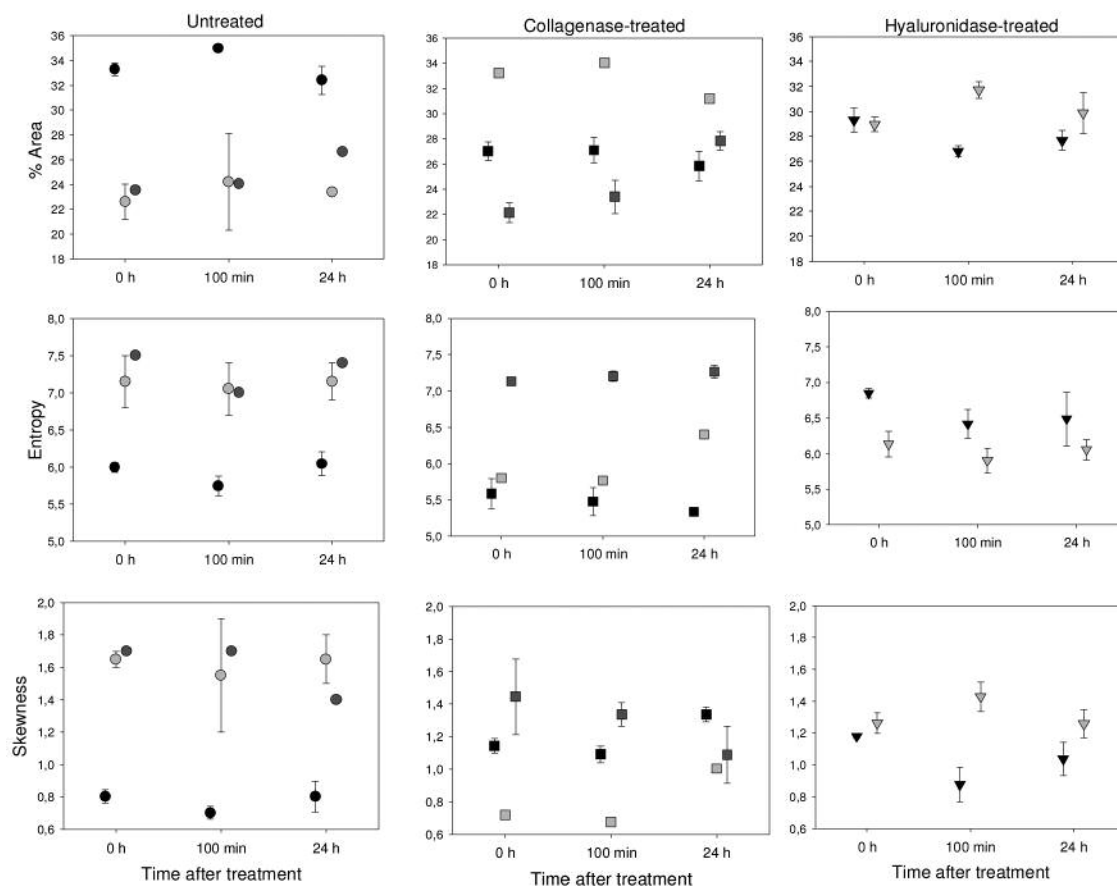
Figure 6. *Analysis of collagen network in tumour tissue growing in dorsal skinfold window chamber. % Area of SHG signal, entropy and skewness values versus imaging time after enzymatic treatment of individual untreated (circles), collagenase- (squares) and hyaluronidase-treated (triangles) mice. Each symbol represents one mouse and 1-4 positions were imaged in each mouse. Bars=standard error.*

lower skewness value. The lower skewness value is due to a more symmetrically distributed intensity histogram from images collected from the dorsal skinfold window chambers, reflecting that the collagen fibres were more evenly spread in these images compared to collagen in frozen sections. The significant differences in skewness found in frozen sections, with an overall reduced skewness 24 h after collagenase treatment, could be indicative of increased collagen content also reflected in differences in % area SHG signal.

The main reason for no detectable visible effects and no effect on collagen content and structure is most likely due to too low a sensitivity in the detection of SHG signal and too low a lateral resolution. The diffraction-limited resolution was approximately 600 nm, which is at the fibrillar level. Collagen is organized in structures such as microfibrils (4-8 nm), fibrils (10-500 nm) and fibres (1-500 μm) after an initial alignment of the triple helical molecules ~300×1.5 nm (31, 32). Another study of the collagen network in dorsal window chambers demonstrated

no changes in collagen fibre length, although the SHG signal intensity decreased (33), indicating some structural changes of collagen fibrils (34, 35).

Considering the above findings, the macroscopic collagen network seems to be a fairly stable scaffolding both in content and structure, despite *i.v.* injection of degrading enzymes. However, some microscopic changes must obviously have occurred affecting uptake and distribution of therapeutic molecules.

Clinical implications. The present study directly compares for the first time the effect of collagenase and hyaluronidase on the uptake and distribution of a liposome-encapsulated small drug (doxorubicin) and a macromolecule (IgG). Although the effect presented is rather small, there is a clear indication that collagenase treatment is more efficient in delivery of larger molecules than hyaluronidase. Both enzymes increase the diffusion of macromolecules (20, 21), induce a transcapillar pressure gradient (4, 12), and influence

transient perfusion (36), while collagenase was shown to have the highest impact on both diffusion and transient perfusion. However, administration of collagenase represents a clinical problem. Collagenase belongs to the MMP family with many members shown to promote tumour growth, invasion and metastasis (37, 38). There may be certain MMPs which do not stimulate metastasis. The collagenase MMP-8 is one such candidate; it was also shown to improve the distribution of oncolytic viruses (39).

There should thus be a focus on MMPs to be used clinically in combination with large novel therapeutic molecules, whereas hyaluronidase, which already demonstrated clinical advantages adjuvant with chemotherapy, should be given in combination with small free or encapsulated drugs.

Acknowledgements

References

1 Jain RK: Transport of molecules in the tumor interstitium – A review. Cancer Res *47*: 3039-3051, 1987.

2 Boucher Y, Baxter LT and Jain RK: Interstitial pressure-gradients in tissue-isolated and subcutaneous tumors – implications for therapy. Cancer Res *50*: 4478-4484, 1990.

3 Boucher Y and Jain RK: Microvascular pressure is the principal driving force for interstitial hypertension in solid tumors – implications for vascular collapse. Cancer Res *52*: 5110-5114, 1992.

4 Eikenes L, Bruland ØS, Brekken C and Davies C de L: Collagenase increases the transcapillary pressure gradient and improves the uptake and distribution of monoclonal antibodies in human osteosarcoma xenografts. Cancer Res *64*: 4768-4773, 2004.

5 Netti PA, Berk DA, Swartz MA, Grodzinsky AJ and Jain RK: Role of extracellular matrix assembly in interstitial transport in solid tumors. Cancer Res *60*: 2497-2503, 2000.

6 Jain RK: Delivery of molecular and cellular medicine to solid tumors. Adv Drug Deliv Rev *46*: 149-168, 2001.

7 Pluen A, Boucher Y, Ramanujan S, McKee TD, Gohongi T, di Tomaso E, Brown EB, Izumi Y, Campbell RB, Berk DA and Jain RK: Role of tumor–host interactions in interstitial diffusion of macromolecules: Cranial *vs.* subcutaneous tumors. Proc Natl Acad Sci USA *98*: 4628-4633, 2001.

8 Davies CdeL, Berk DA, Pluen A and Jain RK: Comparison of IgG diffusion and extracellular matrix composition in rhabdomyosarcomas grown in mice *versus in vitro* as spheroids reveals the role of host stromal cells. Br J Cancer *86*: 1639-1644, 2002.

9 Choi J, Credit K, Henderson K, Deverkadra R, He Z, Wiig H, Vanpelt H and Flessner MF: Intraperitoneal immunotherapy for metastatic ovarian carcinoma: Resistance of intratumoral collagen to antibody penetration. Clin Cancer Res *12*: 1906-1912, 2006.

10 Levick JR: Flow through interstitium and other fibrous matrices. Q J Exp Physiol *72*: 409-438, 1987.

11 Brekken C, Hjelstuen MH, Bruland ØS and Davies C de L: Hyaluronidase-induced periodic modulation of the interstitial fluid pressure increases selective antibody uptake in human osteosarcoma xenografts. Anticancer Res *20*: 3513-3519, 2000.

12 Eikenes L, Tari M, Tufto I, Bruland ØS and Davies C de L: Hyaluronidase induces a transcapillary pressure gradient and improves the distribution and uptake of liposomal doxorubicin (Caelyx™) in human osteosarcoma xenografts. Br J Cancer *93*: 81-88, 2005.

13 Mok W, Boucher Y and Jain RK: Matrix metalloproteinases-1 and -8 improve the distribution and efficacy of an oncolytic virus. Cancer Res *67*: 10664-10668, 2007.

14 Fodstad Ø, Brøgger A, Bruland ØS, Solheim ØP, Nesland JM and Pihl A: Characteristics of a cell-line established from a patient with multiple osteosarcoma, appearing 13 years after treatment for bilateral retinoblastoma. Int J Cancer *38*: 33-40, 1986.

15 Brekken C, Bruland ØS and Davies C de L: Interstitial fluid pressure in human osteosarcoma xenografts: Significance of implantation site and the response to intratumoral injection of hyaluronidase. Anticancer Res *20*: 3503-3512, 2000.

16 Endrich B, Asaishi K, Gotz A and Messmer K: Technical report – a new chamber technique for micro-vascular studies in unanesthetized hamsters. Res Exp Med *177*: 125-134, 1980.

17 Bruland ØS, Fodstad Ø, Stenwig AE and Pihl A: Expression and characteristics of a novel human osteosarcoma-associated cell-surface antigen. Cancer Res *48*: 5302-5309, 1988.

18 Erikson A, Örtegren J, Hompland T, Davies C de L and Lindgren M: Quantification of the second-order nonlinear susceptibility of collagen I using a laser scanning microscope. J Biomed Optics *12*: 044002-1-044002-10, 2007.

19 Gonzalez RC, Woods RE and Eddins SL: *In*: Digital Image Processing Using Matlab. Pearson Prentice Hall, Upper Saddle River, NJ, pp. 464-468, 2004.

20 Davies CdeL, Lundstrøm LM, Frengen J, Eikenes L, Bruland ØS, Kaahus O, Hjelstuen MHB and Brekken C: Radiation improves the distribution and uptake of liposomal doxorubicin (Caelyx™) in human osteosarcoma xenografts. Cancer Res *64*: 547-553, 2004.

21 Alexandrakis G, Brown EB, Tong RT, McKee TD, Campbell RB, Boucher Y and Jain RK: Two-photon fluorescence correlation microscopy reveals the two-phase nature of transport in tumors. Nat Med *10*: 203-207, 2004.

22 McKee TD, Grandi P, Mok W, Alexandrakis G, Insin N, Zimmer JP, Bawendi MG, Boucher Y, Breakefield XO and Jain RK: Degradation of fibrillar collagen in a human melanoma xenograft improves the efficacy of an oncolytic herpes simplex virus vector. Cancer Res *66*: 2509-2513, 2006.

23 Erikson A, Andersen HN, Naess SN, Sikorski P and Davies C de L: Physical and chemical modifications of collagen gels: Impact on diffusion. Biopolymers *89*: 135-143, 2008.

24 Kohno N, Ohnuma T and Truog P: Effects of hyaluronidase on doxorubicin penetration into squamous carcinoma multicellular tumor spheroids and its cell lethality. J Cancer Res Clin Oncol *120*: 293-297, 1994.

25 Baumgartner G: Hyaluronidase in the management of malignant diseases. Wien Klin Wochenschr *99*: 3-22, 1987.

26 Maier U and Baumgartner G: Metaphylactic effect of mitomycin-c with and without hyaluronidase after transurethral resection of bladder-cancer – Randomized trial. J Urol *141*: 529-530, 1989.

27 Smith KJ, Skelton HG, Turiansky G and Wagner KF: Hyaluronidase enhances the therapeutic effect of vinblastine in intralesional treatment of Kaposi's sarcoma. J Am Acad Dermatol *36*: 239-242, 1997.

28 Bookbinder LH, Hofer A, Haller MF, Zepeda ML, Keller A, Lim JE, Edgington TS, Shepard HM, Patton JS and Frost GI: A recombinant human enzyme for enhanced interstitial transport of therapeutics. J Controlled Release *114*: 230-241, 2006.

29 Davies CdeL, Rønning LM and Eikenes L: Proceedings 95th Annual Meeting of the Am Assoc for Cancer Res, Orlando, Florida. Cadmus Professional Comm p. 277, 2004.

30 Henry CBS and Duling BR: Permeation of the luminal capillary glycocalyx is determined by hyaluronan. Am J Physiol Heart Circ Physiol *277*: H508-H514, 1999.

31 Olsen BR: Collagen biosynthesis. *In*: Cell Biology of Extracellular Matrix. Second edition. Hay ED (ed.). Plenum Press, New York, pp. 177-220, 1991.

32 Hulmes DJS: Building collagen molecules, fibrils, and suprafibrillar structures. J Struct Biol *137*: 2-10, 2002.

33 Brown E, McKee T, diTomaso E, Pluen A, Seed B, Boucher Y and Jain RK: Dynamic imaging of collagen and its modulation in tumors *in vivo* using second-harmonic generation. Nat Med *9*: 796-800, 2003.

34 Stoller P, Celliers PM, Reiser KM and Rubenchik AM: Quantitative second-harmonic generation microscopy in collagen. Appl Opt *42*: 5209-5219, 2003.

35 Williams RM, Zipfel WR and Webb WW: Interpreting second-harmonic generation images of collagen I fibrils. Biophys J *88*: 1377-1386, 2005.

36 Tufto I, Hansen R, Byberg D, Nygaard K, Tufto J and Davies C de L: The effect of collagenase and hylaronidase on transient perfusion in human osteosarcoma xenografts grown orthotopically in dorsal skinfold chambers. Anticancer Res *27*: 1475-1482, 2007.

37 Brinckerhoff CE and Matrisian LM: Timeline – Matrix metalloproteinases: A tail of a frog that became a prince. Nat Rev Mol Cell Bio *3*: 207-214, 2002.

38 Stamenkovic I: Extracellular matrix remodelling: The role of matrix metalloproteinases. J Pathol *200*: 448-464, 2003.

39 Montel V, Kleeman J, Agarwal D, Spinella D, Kawai K and Tarin D: Altered metastatic behavior of human breast cancer cells after experimental manipulation of matrix metalloproteinase-8 gene expression. Cancer Res *64*: 1687-1694, 2004.